STEM CELLS®

TISSUE-SPECIFIC STEM CELLS

Modeling of Aniridia-Related Keratopathy by CRISPR/Cas9 Genome Editing of Human Limbal Epithelial Cells and Rescue by Recombinant PAX6 Protein

LAURIANE N. ROUX,[a,b] ISABELLE PETIT,[a,b] ROMAIN DOMART,[c] JEAN-PAUL CONCORDET,[c] JIEQIONG QU,[d,e] HUIQING ZHOU,[d,e] ALAIN JOLIOT,[f] OLIVIER FERRIGNO,[g] DANIEL ABERDAM [a,b]

Key Words. PAX6 • Aniridia-related keratopathy • Limbal stem cells • CRISPR/Cas9 • Recombinant protein

ABSTRACT

Heterozygous *PAX6* gene mutations leading to haploinsufficiency are the main cause of congenital aniridia, a rare and progressive panocular disease characterized by reduced visual acuity. Up to 90% of patients suffer from aniridia-related keratopathy (ARK), caused by a combination of factors including limbal epithelial stem cell (LSC) deficiency, impaired healing response and abnormal differentiation of the corneal epithelium. It usually begins in the first decade of life, resulting in recurrent corneal erosions, sub-epithelial fibrosis, and corneal opacification. Unfortunately, there are currently no efficient treatments available for these patients and no in vitro model for this pathology. We used CRISPR/Cas9 technology to introduce into the *PAX6* gene of LSCs a heterozygous nonsense mutation found in ARK patients. Nine clones carrying a p.E109X mutation on one allele were obtained with no off-target mutations. Compared with the parental LSCs, heterozygous mutant LSCs displayed reduced expression of PAX6 and marked slow-down of cell proliferation, migration and detachment. Moreover, addition to the culture medium of recombinant PAX6 protein fused to a cell penetrating peptide was able to activate the endogenous *PAX6* gene and to rescue phenotypic defects of mutant LSCs, suggesting that administration of such recombinant PAX6 protein could be a promising therapeutic approach for aniridia-related keratopathy. More generally, our results demonstrate that introduction of disease mutations into LSCs by CRISPR/Cas9 genome editing allows the creation of relevant cellular models of ocular disease that should greatly facilitate screening of novel therapeutic approaches.

STEM CELLS *2018;36:1421–1429*

SIGNIFICANCE STATEMENT

Mutations on the *PAX6* gene are responsible for aniridia syndrome that results in a limbal stem cell deficiency-like disorder of the cornea, called aniridia-related keratopathy (ARK). There is no treatment available for these patients and no cellular models for therapeutic drug screening. By genome editing on limbal epithelial cells, a unique cellular model that recapitulates ARK phenotype and is rescued by soluble recombinant PAX6 protein has been produced. It suggests that administration of such recombinant PAX6 protein could be a promising therapeutic approach of congenital aniridia. Moreover, the cellular model will be of great value for drug screening.

INTRODUCTION

The cornea, which is the outermost tissue of the eye, serves as a barrier against external insults and plays an optic role as a major light focusing structure. The corneal epithelium rests on a fibroblast stromal layer and is renewed by limbal epithelial stem cells (LSCs) that are located at the corneal/conjunctival transition zone, known as the limbus [1]. Loss of corneal transparency is frequently caused by aniridia, a bilateral panocular rare disease with an incidence of 1:64,000–1:96,000 [2]. This mainly inherited disease (2:3 of cases, 1:3 sporadic cases) is caused in 90% of aniridic patients by mutations related to *PAX6* gene, the master gene of eye development [3]. The majority of these mutations are nonsense mutations, which generate premature termination codons that result in haploinsufficiency and thus abolish the production of PAX6 protein due to nonsense-mediated mRNA decay [2]. The reduced level of

[a]INSERM U976, Hôpital Saint-Louis, Paris, France; [b]Université Paris-Diderot, Sorbonne Paris Cité, Paris, France; [c]INSERM U1154, CNRS UMR 7196, Museum National d'Histoire Naturelle, Paris, France; [d]Department of Human Developmental biology, Radboud University, Nijmegen, The Netherlands; [e]Faculty of Sciences, Department of Human Genetics, Radboud University Nijmegen, The Netherlands; [f]Collège de France CNRS/UMR 7241 - INSERM U1050; [g]UMRS 938, Centre de Recherche Saint-Antoine, Paris, France

Correspondence: Daniel Aberdam, Ph.D., INSERM U976. Telephone: 33153722071; e-mail: daniel.aberdam@inserm.fr Postal address : Hôpital Saint-Louis, Equerre Bazin, 1 avenue Claude Vellefaux, 75010 Paris, France

Received January 10, 2018; accepted for publication May 14, 2018; first published online in STEM CELLS *EXPRESS* May 29, 2018.

http://dx.doi.org/10.1002/stem.2858

PAX6 protein leads to several ocular deficits including iris hypoplasia, cataracts, fovea and optic nerve dysplasia, glaucoma and most prominently, the severe corneal phenotype of aniridia-related keratopathy (ARK) characterized by conjunctival cell ingrowth, corneal neo-vascularization and opacity with eventual visual loss [4].

Complete ablation of the *Pax6* gene in different organisms leads to a failure in eye formation while *Pax6* heterozygous mice display a small eye phenotype and thus does not fully recapitulate human disease [5–8]. Despite the documentation of corneal phenotypes in *Pax6* mutants, the gene network regulated by PAX6 in healthy cornea remains poorly known [9,10]. It has been speculated that the limbal niche is dysfunctional in eyes of *Pax6* heterozygous mice [5].

So far no specific drugs or efficient treatments are available for aniridic patients. Among them, cultured autologous oral mucosal epithelial transplantation (COMET) is a promising technique with variable outcomes [11]. Moreover, it has been shown that ataluren can rescue some aniridia defects but, as mice do not present opacification like humans, there is no possibility to study ataluren efficacy for ARK [12]. Therefore, the medical need justifies the development of novel cellular models and therapeutic strategies.

Here we report the creation, characterization and rescue of the first cellular model of *PAX6* haploinsufficiency in immortalized LSCs. We introduced by genome editing with CRISPR/Cas9 a point mutation encoding a nonsense mutation p.E109X (c.687 G > T) carried by patients with ARK phenotype [2]. The mutated cells display altered PAX6 expression as well as reduced cell proliferation, migration, and detachment. We further demonstrate that soluble recombinant PAX6 protein added into the culture medium is able to activate its endogenous expression and to rescue the mutated cells phenotype. It suggests that recombinant PAX6 protein could become a therapeutic tool for aniridia patients but overall validates this ARK model, as a tool to identify crucially needed therapeutic tools through drug screening.

Materials and Methods

Cells and Culture Conditions

Human telomerase-immortalized limbal epithelial stem cells (T-LSCs), obtained from J. Rheinwald (Boston), were cultured, as described earlier [13], in Keratinocyte serum-free medium (K-sfm) (Gibco, Life Technologies, Carlstad, CA, USA), supplemented with 25 μg/ml Bovine Pituitary Extract (BPE; Gibco, Life Technologies), 0.2 ng/ml Epidermal Growth Factor (EGF, Peprotech, Neuilly-sur-Seine, France), 0.4 mM $CaCl_2$, 2 mM Glutamine (Gibco, Life Technologies), and 100 U/ml Penicillin/Streptomicin (Gibco, Life Technologies). *PAX6*$^{+/-}$ T-LSCs were cultured in the same conditions. Routine subcultures were obtained by detaching cells with StemPro Accutase Cell Dissociation Reagent (Gibco, Life Technologies) and replating at 2,000 cells/cm^2 (T-LSCs) or 3,000 cells/cm^2 (*PAX6*$^{+/-}$ T-LSCs). Primary LSCs and corneal fibroblasts (COFs) were cultivated as described elsewhere [14,15]. All cells were negative for mycoplasma contamination (monthly tested).

Genome Editing of T-LSCs with CRISPR/Cas9 System

The homology arms were synthesized as G-blocks (Integrated DNA technologies, Leuven, Belgium) based on the *PAX6* genome sequence available from hg38; 5′ homology was chr11:31,800,976-31,802,275 with a single point mutation G > T at position chr11:31,801,593–31,801,593 and 3′ homology arm was chr11:31,800,676–31,801,476. The selection cassette was flanked by FRT sites to allow removal of the puromycin resistance cassette. We have chosen to introduce the point mutation responsible for a premature STOP codon p.E109X, carried by two patients monitored clinically as ARK [2]. A guide RNA sequence targeting the intron downstream of the corresponding coding exon was cloned into pMLM3636 expression plasmid (targeted sequence, with guide RNA spacer sequence in uppercase and PAM in lowercase 5′-GACACAGACTAAGAGACAGGtgg-3′). Guide RNA activity was checked by the T7 assay after cotransfection of guide RNA and Cas9 expression plasmids before using it to drive KI of the p.E109X point mutation. A donor plasmid was constructed with a puromycine resistance cassette flanked by approximately 1,000 bp homology arms to sequence flanking the DNA cleavage site directed by guide. The 5′ homology arm sequence contained the p.E109X point mutation and was expected to be introduced during homology-dependent repair (HDR)-mediated repair of guide/Cas9-mediated DNA cleavage copying from the plasmid donor template. Guide RNA and Cas9 expression plasmids were cotransfected together with the donor plasmid into LSCs using the Human Keratinocyte Nucleofector Kit and optimized program T-007 (Amaxa, Lonza, Bâle, Switzerland). Then the cells were seeded at low dilution in 150 mm culture dishes. As inserting a *PAX6* nonsense mutation could modulate cell survival/proliferation/fate, we screened for KI clones with 10 μg/ml puromycin and let all resistant clones (even the slower growing ones) appear and be amplified. Genomic DNA was extracted from the 120 isolated clones following manufacturers' instructions (E.Z.N.A. Tissue DNA kit, Omega Bio-tek). All the clones were then tested using specific PCR amplification of the mutated allele. Primers sequences used are presented in Supporting Information Table SI. Several potential off-target sites for the guide RNA were identified with CRISPOR software [16], amplified by PCR using specific primers (Supporting Information Table SI) and sequenced. High throughput methods would be required to more thoroughly whether off-target mutations are present in the clones or could be detected at low frequency in the cells transfected with guide RNA and Cas9 expression plasmids.

Rescue Experiments

PAX6$^{+/-}$ T-LSCs were treated as specified below with 2 μg/ml recombinant PAX6 protein coupled with an 11R-tag (recPAX6, LD Biopharma Inc, San Diego, CA, USA) directly added into the culture medium. This dose was determined following manufacturers' instructions and preliminary Reverse Transcription quantitative Polymerase Chain Reaction (RT-qPCR) data obtained on T-LSCs showing that the highest PAX6 transcriptional induction was obtained with 2 μg/ml recPAX6 (range from 0.5 μg/ml to 4 μg/ml, *data not shown*). In parallel, T-LSCs and *PAX6*$^{+/-}$ T-LSCs were treated with the buffer (confidential composition) used to dilute recPAX6 as control condition. The sequence of recPAX6 encodes for the full PAX6 canonical isoform (isoform a) coupled with a C-term 29aa-tag including the 11R tag (LEESGGGGSPGRRRRRRRRRRR).

qRT-PCR Analysis

Cells were treated for 10 hours with either 2 μg/ml recPAX6 or its buffer (control) for rescue experiments, and harvested as a dry pellet. RNA was then extracted using RNEasy Mini kit (QIAGEN, Hilden, Germany) and cDNA were synthetized from 1 μg RNA using iScript cDNA synthesis kit (Bio-Rad, Hercules, CA, USA). Quantitative PCR were performed in triplicate using 2X SYBR Green PCR Master Mix (Absource Biotools, Munich, Germany). Expression of each gene was calculated using the $2^{-\Delta\Delta Ct}$ method. Results are presented as fold change normalized to B2M house-keeping gene and relative to control (treated with protein buffer or untreated) T-LSCs. Specific primers sequences used are listed in Supporting Information Table SI.

Immunofluorescence Staining

Cells were seeded on 0.1% gelatin-coated coverslips in 24-well at 5,400 cells (primary LSCs and T-LSCs) or 7,500 cells ($PAX6^{+/-}$ T-LSCs) per well. They were fixed three days after with 4% paraformaldehyde for 20 minutes at room temperature, incubated for 10 minutes in glycine 1 mM to quench PFA and permeabilized, for nuclear antibodies, with 0,5% Triton X-100 in $DPBS^{+/+}$ (Gibco, Life Technologies) for 7 minutes, with 3 × 5 minutes of washing in $DPBS^{+/+}$ between each step. After blocking in 5% BSA for 30 minutes, cells were incubated with primary antibodies overnight at 4°C in humidified atmosphere. Primary antibodies used were against PAX6 (ab2237, 1/800, Millipore, Burlington, MA, USA), KRT14 (905301, 1/500, BioLegend, San Diego, CA, USA), p63 (ab735, 1/50, Abcam), KRT3 (CBL218, 1/100, Millipore), KRT12 (sc17101, 1/20, Santa Cruz Biotechnology Inc., Dallas, TX, USA), Connexin43 (CX43, BD610061, 1/400, BD Biosciences, Franklin Lakes, NJ, USA), and E-cadherin (CDH1, MAB1838, 1/100, R&D Systems, Minneapolis, MN, USA). Cells were washed in $DPBS^{+/+}$ and incubated with corresponding secondary antibodies: goat anti-rabbit AlexaFluor 488, goat anti-mouse and donkey anti-goat AlexaFluor 594 (Life Technologies) diluted at 1/3,000 or goat anti-rabbit AlexaFluor 594 (Life Technologies) diluted at 1/2,000 in blocking buffer for 1 hour at room temperature protected from light. Coverslips were finally washed, mounted on microscope slides (DAPI fluoromount-G, Electron Microscopy Sciences, Hatfield, PA, USA) and visualized under a Nikon Eclipse Ti epifluorescence microscope equipped with an OrcaFlash 4.0 LT camera (Hamamatsu). Picture analyses were conducted using NIS-Elements software.

Western Blot Analysis

Cells were harvested as a dry pellet, after 16 hours or 24 hours of treatment with 2 μg/ml recPAX6 protein or its buffer for rescue experiments, lysed in RIPA buffer supplemented with Protease and Phosphatase Inhibitor Cocktail EDTA-Free (Roche, Bâle, Switzerland) for 15 minutes on ice and centrifuged for 15 minutes at 4°C at 15,000 *g*. Protein concentration was measured using Pierce BCA Protein Assay kit (Thermo Fisher Scientific, Waltham, MA, USA) following manufacturer instructions. Thirty micrograms of total protein or 10 ng of recPAX6 protein were loaded on a SDS-PAGE gel (10%), transferred to nitrocellulose membranes using semi-dry method. Membranes were prestripped using Re-Blot Plus Strong solution (EMD Millipore) for 15 minutes, blocked twice for 5 minutes in 5% milk solution and incubated in primary antibody (PAX6, ab2237, Millipore, 1/1,000) overnight at 4°C. After three washing of 10 minutes in Tris-buffered saline (TBS) with 0.2% Tween (TBS-T), membranes were incubated for 1 hour with secondary antibody (Goat anti-rabbit HRP, BD Biosciences) diluted in TBS-T 5% milk solution at 1/1,000. Proteins were visualized using chemiluminescence detection (Clarity Western ECL Substrate, Bio-Rad) on a gel imaging system (ImageQuant LAS 4000). Membranes were stripped again, incubated 90 minutes at room temperature with ACTIN (sc1615, 1/500, Santa Cruz) antibody diluted in TBS-T 5% milk, washed 3 times 10 minutes in TBS-T and incubated for 1 hour in secondary antibody (Rabbit anti-goat HRP, 1/20,000, Jackson ImmunoResearch) at room temperature before revelation. Signal quantifications were made using ImageJ 1.49 software (NIH). Results are presented after ACTIN normalization.

TRE-PAX6-Luc Reporter Assay

Wild-type (WT) and $PAX6^{+/-}$ T-LSCs were transfected in triplicates with Fugene HD Transfection Reagent (Promega, Madison, WI, USA) and TRE-PAX6-Luciferase construct (TRE-PAX6-luc) or control plasmids (Cignal PAX6 Reporter Assay kit, Qiagen) to a ratio of 3 to 1, and seeded at 5,000 (T-LSCs) and 6,500 ($PAX6^{+/-}$ T-LSCs) cells per well into 96-well plates. Culture medium was changed 24 hours after and on day 2, cells were incubated with 2 μg/ml recPAX6 protein or its buffer (untreated control) during 3 hours and 30 minutes before cell lysis. Firefly (TRE signal) and Renilla (internal control) luciferase activities were then measured sequentially following manufacturers' instructions (Dual-Luciferase Reporter Assay system, Promega) and using a luminometer microplate reader FLUOstar Omega (BMG Labtech). Results are presented after normalization with Renilla activity.

Cell Proliferation

WT and mutant T-LSCs were seeded into 96-well plates at 500 cells per well in six replicates. Three days later, a tetrazolium compound was added directly into the cells culture medium (CellTiter 96, Promega) and incubated for 3 hours. Absorbance was then recorded at 490 nm indicating the quantity of formazan product and thus the proliferation rate.

RNA-Seq Analysis

WT and $PAX6^{+/-}$ T-LSCs #2 cells were harvested as a dry pellet and RNA was extracted using RNEasy Mini kit with gDNA eliminators columns (QIAGEN). RNA-Seq experiment was performed as described previously [17] with the starting material of 500 ng total RNA (n = 2 for each cell type), to obtain double-strand cDNA (ds-cDNA). After purification with the MinElute Reaction Cleanup Kit (28206, QIAGEN), 3 ng ds-cDNA was processed for library construction using KAPA Hyper Prep Kit (KK8504, KAPA Biosystems, Roche) according to the standard protocol except that a 15 minutes USER enzyme (M5505L, NEB, Ipswich, MA, USA) incubation step was added before library amplification. The prepared libraries were quantified with the KAPA Library Quantification Kit (KK4844, KAPA Biosystems, Roche), and then sequenced in a paired-ended manner using the NextSeq 500 (Illumina) according to standard Illumina protocols. Approximately 15–25 × 10^6 reads were sequenced for each sample. Sequencing reads were aligned to human genome assembly hg19 (NCBI version 37) using STAR 2.5.0 with default options. For data visualization, wigToBigWig from the UCSC genome browser tools was used to generate bigwig files and uploaded to UCSC genome browser. Genes with the mean of DESeq2-normalized counts ("baseMean") > 10 are considered

to be expressed [18]. Differential gene expression (non-adjusted p-value < .001) was further analyzed. Functional gene ontology annotation of genes was performed with DAVID [19].

In Vitro Migration Test

WT and *PAX6*$^{+/-}$ T-LSCs were seeded into culture-inserts 2 well at 25,000 cells per well in 6-well plates (ibidi, Martinsried, Germany). After adhesion, cells were treated with either 2 μg/ml recPAX6 or its buffer (control) for rescue experiments. Sixteen hours after plating, the inserts were removed creating a gap of 500 μm between cells. Patches were overlaid with culture medium and closure of the gap was monitored for 10 hours, taking pictures at regular time intervals. Gap width was measured using ImageJ 1.49 software (NIH). Results are presented as percent of gap width normalized at 100% at t = 0 hour.

Detachment Assay

Cells were seeded in 6-well plates and treated for 10 hours with recPAX6 at 2 μg/ml or its buffer in rescue experiments. Then, cells were incubated in StemPro Accutase Cell Dissociation Reagent and detached cells were removed after 8 minutes. Fresh accutase was added for 8 more minutes and detached cells were collected. Finally, cells were incubated 6 minutes in fresh accutase to harvest all the remaining cells. The three collected cells fractions (detached after 8, 16, or 22 minutes) were counted and results were normalized to the total number of detached cells (100%).

Statistical Analysis

Data are expressed as means +/- SEM, except for Gene Ontology charts as indicated, and analyzed by Prism v7.04 (GraphPad software, Inc). Normality was first evaluated using Shapiro-Wilk test. Then, unpaired t test (T-LSCs vs. PAX6$^{+/-}$ T-LSCs experiments), one-way ANOVA (analysis of variance) followed by multiple comparison Dunnett's test (rescue experiments, proliferation and WB figures) or two-way ANOVA followed by Bonferroni's test (migration assays) were performed, as indicated in legends, to calculate p-values. Differences are considered to be statistically significant from a p-value below .05.

Results and Discussion

Gene Editing of ARK Mutation by CRISPR/Cas9 in Limbal Cells

Performing cornea biopsies on patients with aniridia would increase the risk of aggravating the disease and it is therefore barely possible to extract and amplify disease-related limbal or corneal cells [20]. On the other hand, primary healthy LSCs reach replicative senescence around passage 5–7 and thus cannot be used for CRISPR/Cas9. We thus decided to use human telomerase-immortalized LSCs (T-LSCs) for genome editing. A comparative analysis showed that the T-LSCs behave similarly to primary LSC in terms of cell morphology, and expression of PAX6, limbal specific and negative corneal markers (Supporting Information Fig. S1A–S1C).

To recapitulate in vitro limbal *PAX6* haploinsufficiency, we have chosen to introduce a nonsense mutation p.E109X (c.687 G > T) located in the exon 6 of *PAX6* gene and carried by two patients monitored clinically as ARK [2]. For this purpose, a guide RNA targeting DNA cleavage by Cas9 to intron 7 was cotransfected in T-LSCs with Cas9 expression plasmid and a donor plasmid carrying a Puro^{R} cassette flanked by 5′ and 3′ homology arms to the cleavage site. The 5′ homology arm differed from the WT *PAX6* gene sequence by the presence of the 687 G > T mutation and the latter was therefore expected to be introduced into the locus during homology-dependent repair (HDR) (Fig. 1A). Among 120 Puro^{R} clones, 9 clones carrying the point mutation in one allele have been identified with specific primers (Supporting Information Table SI). Selective PCR amplification of the mutated region (Fig. 1A, 1B) and sequencing of the amplicon (Fig. 1C) confirmed that, for these 9 clones, the knock-in occurred only in one allele of *PAX6.* The relatively low efficiency of HDR in these cells (9 out of 120 × 2 = 240 *PAX6* gene copies corresponding to 3.7%) likely prevented the production of homozygous p.E109X mutant *PAX6* clones, although we cannot rule out that the latter could be lethal in T-LSCs. Potential off-targets were identified by bioinformatic analysis with CRISPOR software [16] and sequenced in these clones (Supporting Information Fig. S1D). No predicted mutation was observed in these sites.

Western blot analysis confirmed that the heterozygous mutant *PAX6* clones, named here *PAX6*$^{+/-}$ T-LSCs, produce reduced amounts of PAX6 protein, although with slight differences of intensity from one clone to another (range between 25%–50% reduction compared with the T-LSCs control) (Fig. 1D). It fits the variable expression and penetrance observed in patients (and mice) carrying identical *PAX6* mutation [7–10]. The phenotypic variability seen between mice is also observed within a single SEY strain [21]. This can even be detected between the two eyes of the same mouse, suggesting a stringent requirement for PAX6 activity to be expressed at specific levels at precise times during development [22–24]. Similarly to control T-LSCs, *PAX6*$^{+/-}$ T-LSCs form packed colonies of small cuboid cells positive for keratin 14 (KRT14) and E-cadherin (CDH1) (Supporting Information Fig. S1E). Cell proliferation rate of *PAX6*$^{+/-}$ T-LSCs clones was reduced compared with controls (Fig. 1E). It fits the observation that cells isolated from corneas of *PAX6*$^{+/-}$ heterozygous mice displayed similar morphology but reduced cell proliferation rate compared with cells extracted from WT mice [25].

Molecular and Functional Characterization of *PAX6*$^{+/-}$ T-LSCs

The genes directly regulated by PAX6 in epithelial limbal stem cells and the resulting biological functions are still largely unknown. To clarify the molecular consequence of *PAX6* haploinsufficiency in LSCs, a comparative RNA-Seq analysis has been performed on a *PAX6*$^{+/-}$ T-LSC clone (#2) that displayed 50% reduction of PAX6 and compared with T-LSCs. A total number of 258 differentially expressed genes were detected using DESeq2 [18] (nonadjusted p-value < .001) (Supporting Information Table SIIA). Among them, 171 were down-regulated and 87 were up-regulated in mutant *PAX6*$^{+/-}$ T-LSC #2, compared with T-LSCs. Based on Gene Ontology (GO) analysis using DAVID Bioinformatics Resources [19], down-regulated genes are involved in diverse biological functions, including lipid metabolism (e.g., *ABCA1*), gene expression and epigenetic regulation (e.g., *PAX6* and *DNMT3B*), exocytosis (e.g., *RAB9A*) and response to retinoic acid (e.g., *PPARG*) (Fig. 2A) (Supporting Information Table SIIB). However, up-regulated genes including *NRCAM, PXDN*, *FBN2, TGFBi*, and *ITGA5* seemed to be specifically enriched for extracellular

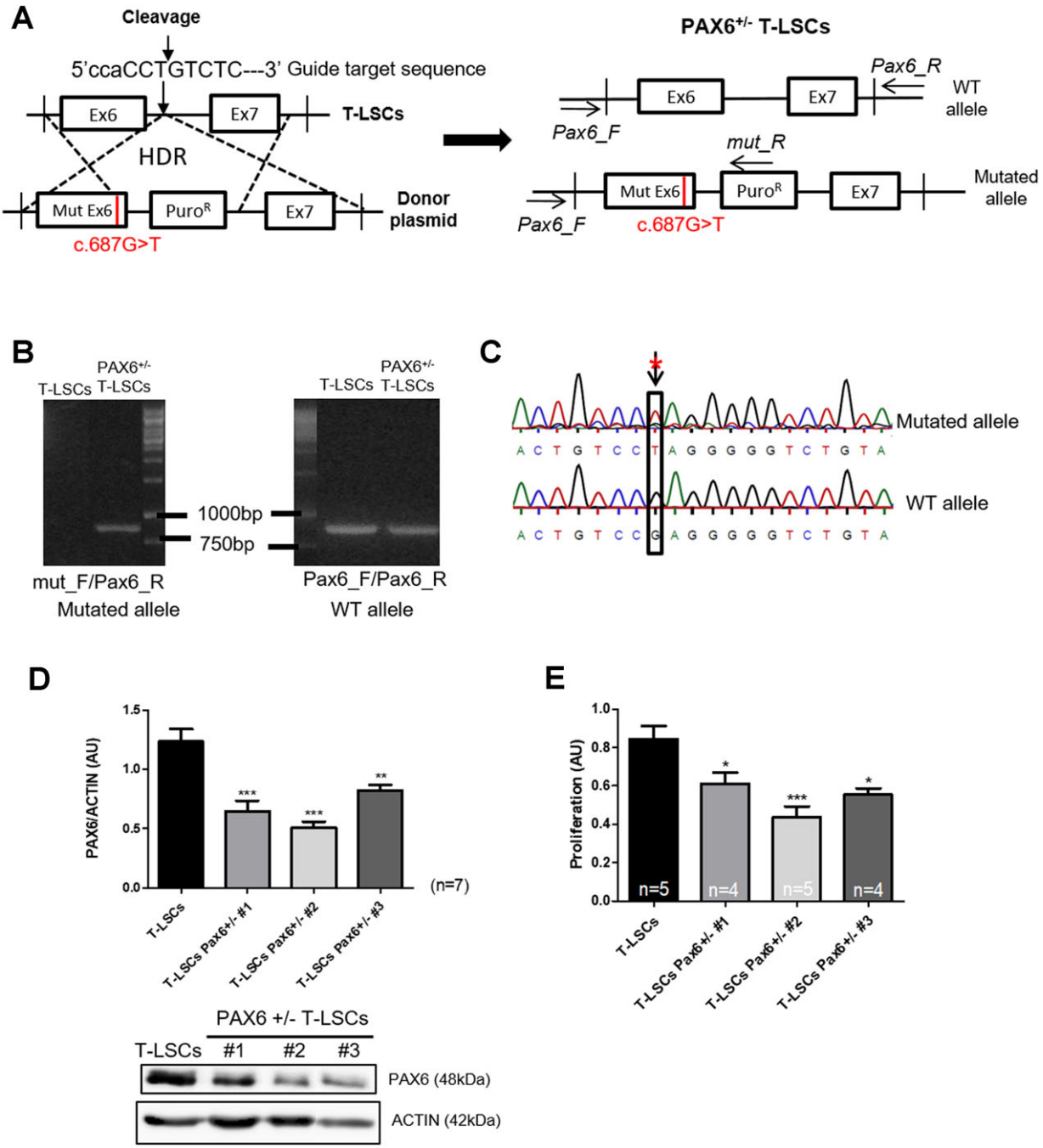

Figure 1. Genome editing with CRISPR/Cas9 system in T-LSCs. **(A)**: Schematic representation of the *PAX6* exon 6 region targeted by the specific guide before HDR with the donor plasmid (left) and after HDR with the primers used for genotyping (right). As the PAM motif (tgg) of the guide RNA used for *PAX6* gene editing is on the noncoding strand of the gene, the cca is indicated (left). The mutation (c.687G > T) is noted in red on the Mut Ex6 and the HDR event is represented by dotted lines (left). **(B)**: Illustration of amplicons of WT and mutated allele obtained for one normal (T-LSCs) and one heterozygous mutated (*PAX6*$^{+/-}$ T-LSC) clone and electrophoresed on 1.2% agarose gel. **(C)**: Sequencing results of PCR amplicons obtained for the WT and the mutated alleles of *PAX6*$^{+/-}$ T-LSCs. **(D)**: Quantification of PAX6 protein expression normalized to ACTIN signal for 3 *PAX6*$^{+/-}$ T-LSCs clones and control cells (n = 7) and representative Western blot below. **(E)**: Proliferation rate quantification measured for T-LSCs and 3 *PAX6*$^{+/-}$ T-LSC clones after 72 hours. (n = 4 or 5 as indicated). One-way ANOVA followed by Dunnett's test: *, p > .05; **, p > .01; ***, p < .001. Abbreviations: cca, complementary motif; HDR, homology-dependent repair; Mut Ex6, mutated exon 6; T-LSCs, telomerase-immortalized limbal epithelial stem cells. [Color figure can be viewed at wileyonlinelibrary.com]

matrix (ECM) organization and cell adhesion (Fig. 2B) (Supporting Information Table SIIC). Accordingly, detachment of *PAX6*$^{+/-}$ T-LSCs with accutase took longer time than for control T-LSCs, suggesting a stronger adhesion of the mutant cells (Fig. 2C). Cell migration and cornea wound healing are altered in aniridic patients [4]. *Pax6*$^{+/-}$ mice present also corneal epithelial cell migration defects [24,25]. Epithelial monolayers cultured from *Pax6*$^{+/-}$ corneal explants in vitro displayed an initial wound healing delay compared with WT cells [8]. Furthermore, in a whole eye culture model, *Pax6*$^{+/-}$ corneas maintained in basal medium

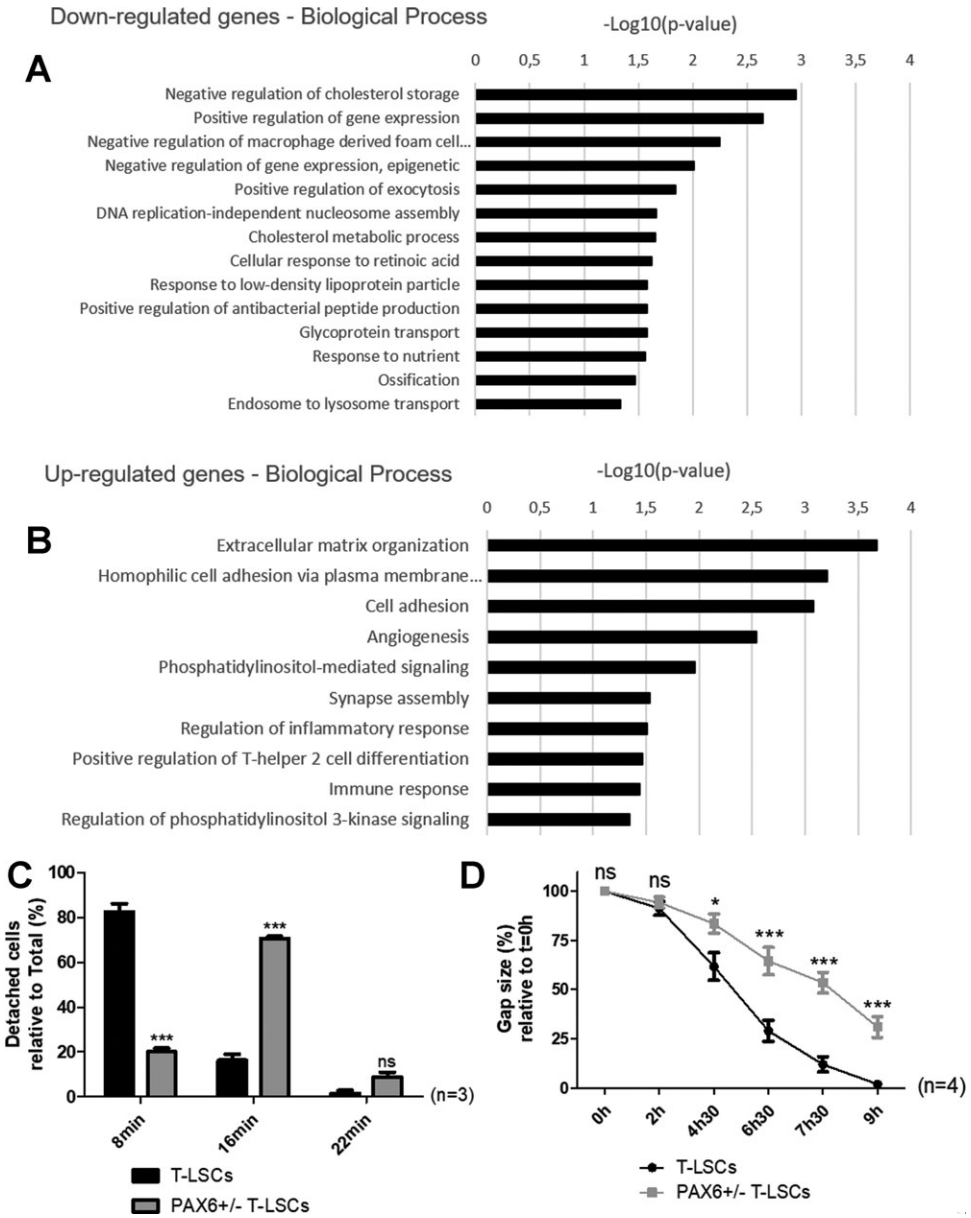

Figure 2. RNA-Seq and functional analysis of *PAX6*$^{+/-}$ T-LSCs. Significant enriched GO biological process terms for **(A)** down-regulated genes and **(B)** up-regulated genes in *PAX6*$^{+/-}$ T-LSCs #2 relative to T-LSCs (n = 2). Significant p-values (p < .05) were transformed by -log 10. **(C)**: Quantification of cells detached in 8 minutes, 16 minutes, and 22 minutes relative to total number of detached cells (100%) for normal and mutated cells (n = 3). One-way ANOVA followed by Dunnett's test: ***, p < .001, ns p > .05. **(D)**: Quantification of gap width normalized at 100% at t = 0 hour monitored in IBIDI migration assay on T-LSCs and *PAX6*$^{+/-}$ T-LSCs (n = 4). Two-way ANOVA followed by Bonferroni's test: *, p < .05; ***, p < .001; and ns p > .05. Abbreviation: T-LSCs, telomerase-immortalized limbal epithelial stem cells.

without any serum or growth factor support show a reduction in wound healing re-epithelialization compared with wild-type [26]. When challenged on ibidi wound chambers, which recapitulate mainly cell migration, gap closure rate was lower with *PAX6*$^{+/-}$ T-LSCs compared with WT cells (Fig. 2D). Reduced migration correlates well with slower proliferation coupled to enhanced adhesion. Therefore, PAX6$^{+/-}$ T-LSCs recapitulate in vitro the human ARK phenotype.

Functional Rescue by Recombinant PAX6 Protein

Autoregulation of PAX6 has been largely described [27–29] and disruption of this self-activation causes aniridia [27]. Proteins that exhibit the unique properties of efficient translocation across cell membrane carry protein transduction domains called cell penetrating peptide (CPP) [30]. We thus tested whether soluble recombinant PAX6 protein carrying 11 arginine (11R) residues as a CPP (recPAX6) could be uptaken by the cells and translocated properly into the nucleus. Addition of recPAX6 (2 μg/ml) into the *PAX6*$^{+/-}$ T-LSCs medium activated the transfected TRE-PAX6-luc construct after 3 hours and 30 minutes, confirming its ability to bind PAX6 activation sites (Fig. 3A). This result strongly suggests that recPAX6 could be biologically active and thus used to rescue *PAX6*$^{+/-}$ T-LSCs.

Moreover, recPAX6 protein restored the transcriptional level of endogenous *PAX6* in PAX6$^{+/-}$ T-LSCs treated 10 hours with soluble PAX6 protein compared with buffer treated cells (Fig. 3B).

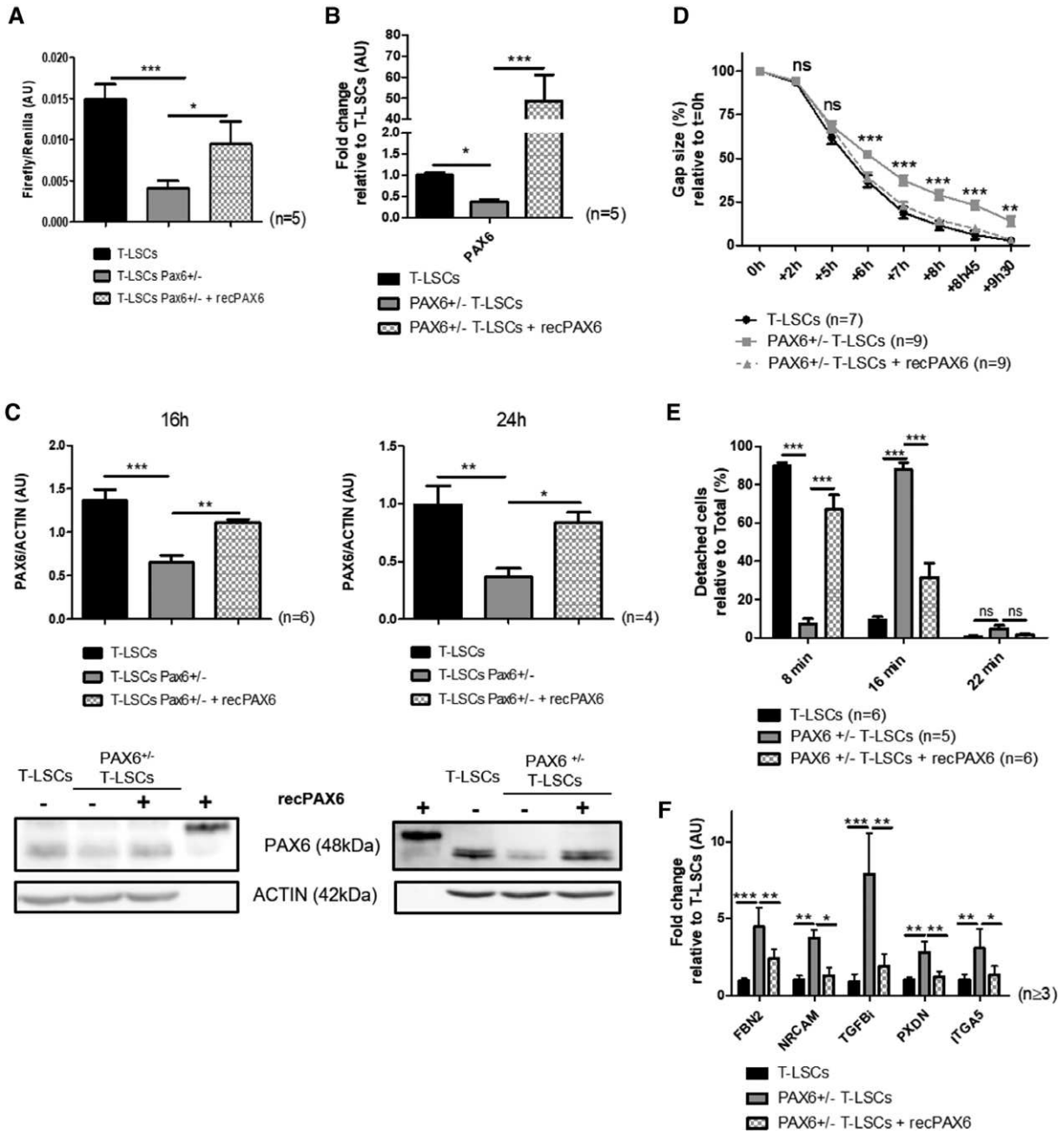

Figure 3. Phenotypic rescue of *PAX6*$^{+/-}$ T-LSCs by recPAX6 protein. **(A)**: Quantification of TRE-binding activity in recPAX6 treated *PAX6*$^{+/-}$ T-LSCs monitored by Firefly:Renilla luciferase activities ratio compared with buffer treated WT and mutated T-LSCs (n = 5). **(B)**: Quantification of PAX6 transcriptional expression after recPAX6 treatment on *PAX6*$^{+/-}$ T-LSCs relative to buffer treated WT and mutated cells (n = 5). **(C)**: Rescue of PAX6 endogenous protein expression (normalized to ACTIN signal) by addition of 2 μg/ml recPAX6 protein on *PAX6*$^{+/-}$ T-LSCs compared with buffer treated cells, revealed by Western blot after 16 hours (n = 6, left) or 24 hours (n = 4, right) of treatment. Representative Western blots below confirm that enhanced PAX6 expression is not due to exogenous tagged recPAX6 (higher band). RecPAX6 rescues also *PAX6*$^{+/-}$ T-LSCs **(D)** migration **(E)** cell detachment and **(F)** up-regulated PAX6 target genes involved in adhesion or ECM organization ($n \geq 3$) compared with buffer treated normal or mutated T-LSCs. One-way ANOVA followed by Dunnett's test was performed for all these experiments but migration assay (two-way ANOVA corrected with Bonferroni's test): *, $p < .05$; **, $p < .01$; ***, $p < .001$, ns $p > .05$. Abbreviation: T-LSCs, telomerase-immortalized limbal epithelial stem cells.

Western blot analysis confirmed the partial restoration of normal PAX6 amount in recPAX6 treated *PAX6*$^{+/-}$ T-LSCs (Fig. 3C). As the recPAX6 contains an 11R-tag, it could be distinguished from the endogenous protein, excluding that the enhanced band contains the exogenous recPAX6 (Fig. 3C). Interestingly, a strong post-transcriptional regulation seems to occur as the mean PAX6 fold change after rescue is around 50 relative to control (Fig. 3B) while protein level appears more physiological (Fig. 3C). This result highlights again the importance of PAX6 dosage.

Furthermore, recPAX6 restored also functional defects of *PAX6*$^{+/-}$ T-LSCs, validating that *PAX6* haploinsufficiency is the main cause of mutated cell phenotype. Indeed, both cell

migration (Fig. 3D and Supporting Information Fig. S1F) and cell detachment (Fig. 3E) of mutant cells returned to normal after treatment with 2 μg/ml recPAX6. From the RNA-Seq analysis, we selected genes involved in adhesion (*NRCAM)*, ECM organization (*PXDN*, *FBN2*) or both (*TGFBi*, *ITGA5*) according to GO terms and whose expression was upregulated by *PAX6* haploinsufficiency in the *PAX6*$^{+/-}$ T-LSCs. Comparative RT-qPCR analyses between cells treated with either recPAX6 or the buffer alone on these genes demonstrate that recPAX6 treatment restored their expression (Fig. 3F). Finally, functional rescue of the cellular phenotype by recPAX6 strongly argues against a role of off target mutations in the phenotype.

The present data strongly confirm that our cellular model recapitulates well the ARK phenotype and the requirement for balanced amount of PAX6. Furthermore, it suggests that recPAX6 could have a potential role in treating ARK or postnatal problems. Major efforts are currently made to use recombinant proteins for clinical use but most proteins do not penetrate the lipid bilayer exterior of mammalian cells, even coupled to CPP-like tag [31]. This severe limitation dramatically limits the number of disease-relevant receptors that proteins can target and modulate. In addition, the risk of protein covalently coupled with CPP, as for recPAX6, is an alteration of the biological activity of the conjugate. It is thus remarkable how recPAX6 could efficiently regulates its own gene expression and rescue the in vitro phenotype of *PAX6*$^{+/-}$ T-LSCs. As PAX6 is also produced in other eye tissues (lens, retina) and also in the pancreas, recPAX6, but also any drug identified with the present model, could be relevant for treating diseases related to these tissues.

Conclusion

In most of the cases, pluripotent stem cells have been used for CRISPR/Cas9 genome editing because of higher efficiency of HDR [32]. The model presented here is, to our knowledge, the first designed by genome editing on LSCs for ocular disease in general and of ARK in particular. The present model will be of great value for a better understanding of ARK physiopathology and to screen for therapeutic drugs.

Acknowledgments

We would like to thank Stéphane Chavanas and Ruby Shalom-Feuerstein for critical reading of the manuscript. This work was supported by grants from Association Française contre les Myopathies (AFM-Téléthon) and Gêniris (French Aniridia patient association), Agence Nationale pour la Recherche (ANR-13-PRTS-0001–02), Fondation pour la Recherche Médicale (FRM team 2014). L.N.R. is a recipient of a PhD fellowship from the French Ministry of Research.

Author Contributions

L.N.R.: conducted most of the experiments, analyzed the results and manuscript writing; I.P.: analyzed the results and provided valuable discussions; R.D. and J.P.C.: designed the CRISPR/Cas9 guide and genome editing strategy; J.Q. and H.Z.: performed and analyzed the comparative RNA-Seq. A.J.: participated to the recombinant protein approach; O.F. and D.A.: conception/design, provided financial support and analyzed the results. D.A.: manuscript writing; L.N.R., I.P., R.D., J.-P.C., J.Q., H.Z., A.J., O.F., D.A.: final approval of manuscript.

Disclosure of Potential Conflicts of Interest

The authors indicated no potential conflicts of interest.

References

1 Pellegrini G, Rama P, Di Rocco A et al. Concise review: Hurdles in a successful example of limbal stem cell-based regenerative medicine. Stem Cells 2014;32:26–34.

2 Robinson DO, Howarth RJ, Williamson KA et al. Genetic analysis of chromosome 11p13 and the PAX6 gene in a series of 125 cases referred with aniridia. Am J Med Genet A 2008;146A:558–569.

3 Axton R, Hanson I, Danes S et al. The incidence of PAX6 mutation in patients with simple aniridia: An evaluation of mutation detection in 12 cases. J Med Genet 1997;34:279–286.

4 Secker GA, Daniels JT. Corneal epithelial stem cells: Deficiency and regulation. Stem Cell Rev 2008;4:159–168.

5 Ramaesh T, Ramaesh K, Martin Collinson J et al. Developmental and cellular factors underlying corneal epithelial dysgenesis in the Pax6+/− mouse model of aniridia. Exp Eye Res 2005;81:224–235.

6 Cvekl A, Callaerts P. PAX6: 25th anniversary and more to learn. Exp Eye Res 2017;156:10–21.

7 Favor J, Gloeckner CJ, Neuhauser-Klaus A et al. Relationship of Pax6 activity levels to the extent of eye development in the mouse, *Mus musculus*. Genetics 2008;179:1345–1355.

8 Dorà N, Ou J, Kucerova R et al. PAX6 dosage effects on corneal development, growth, and wound healing. Dev Dyn 2008;237:1295–1306.

9 Grindley JC, Davidson DR, Hill RE. The role of Pax-6 in eye and nasal development. Development 1995;121:1433–1442.

10 Collinson JM, Quinn JC, Hill RE et al. The roles of Pax6 in the cornea, retina, and olfactory epithelium of the developing mouse embryo. Dev Biol 2003;255:303–312.

11 Shortt AJ, Tuft SJ, Daniels JT. Corneal stem cells in the eye clinic. Br Med Bull 2011;100:209–225.

12 Wang X, Gregory-Evans K, Wasan KM et al. Efficacy of postnatal in vivo nonsense suppression therapy in a Pax6 mouse model of aniridia. Mol Ther Nucleic Acids 2017;7:417–428.

13 Gipson IK, Spurr-Michaud S, Argu et al. Mucin gene expression in immortalized human corneal–limbal and conjunctival epithelial cell lines. Invest Opthalmol Vis Sci 2003;44:2496.

14 Ruby S-F, Laura S, Stephanie DLFD et al. Pluripotent stem cell model reveals essential roles for miR-450b-5p and miR-184 in embryonic corneal lineage specification. Stem Cells 2012;30:898–909.

15 Aberdam E, Petit I, Sangari L et al. Induced pluripotent stem cell-derived limbal epithelial cells (LiPSC) as a cellular alternative for in vitro ocular toxicity testing. PLoS One 2017;12:e0179913.

16 Haeussler M, Schönig K, Eckert H et al. Evaluation of off-target and on-target scoring algorithms and integration into the guide RNA selection tool CRISPOR. Genome Biol 2016;17:

17 Oti M, Kouwenhoven EN, Zhou H. Genome-wide p63-regulated gene expression in differentiating epidermal keratinocytes. Genomics Data 2015;5:159–163.

18 Love MI, Huber W, Anders S. Moderated estimation of fold change and dispersion for RNA-seq data with DESeq2. Genome Biol 2014;15:

19 Huang DW, Sherman BT, Lempicki RA. Systematic and integrative analysis of large gene lists using DAVID bioinformatics resources. Nat Protoc 2009;4:44–57.

20 Latta L, Viestenz A, Stachon T et al. Human aniridia limbal epithelial cells lack expression of keratins K3 and K12. Exp Eye Res 2018;167:100–109.
21 Hill RE, Favor J, Hogan BLM et al. Mouse small eye results from mutations in a paired-like homeobox-containing gene. Nature 1991; 354:522–525.
22 Schedl A, Ross A, Lee M et al. Influence of PAX6 gene dosage on development: Overexpression causes severe eye abnormalities. Cell 1996;86:71–82.
23 van Raamsdonk CD,Tilghman SM. Dosage requirement and allelic expression of PAX6 during lens placode formation. Development 2000;127:5439–5448.
24 Collinson JM, Chanas SA, Hill RE et al. Corneal development, limbal stem cell function, and corneal epithelial cell migration in the *Pax6* $^{+/-}$ mouse. Invest Opthalmol Vis Sci 2004;45:1101.
25 Leiper LJ, Walczysko P, Kucerova R et al. The roles of calcium signaling and ERK1/2 phosphorylation in a Pax6+/- mouse model of epithelial wound-healing delay. BMC Biol 2006;4:27.
26 Ou J, Lowes C, Collinson JM. Cytoskeletal and cell adhesion defects in wounded and Pax6+/− corneal epithelia. Invest Ophthalmol Vis Sci 2010;51:1415–1423.
27 Bhatia S, Bengani H, Fish M et al. Disruption of autoregulatory feedback by a mutation in a remote, ultraconserved PAX6 enhancer causes aniridia. Am J Human Genet 2013;93:1126–1134.
28 Kleinjan DA, Seawright A, Childs AJ et al. Conserved elements in Pax6 intron 7 involved in (auto)regulation and alternative transcription. Dev Biol 2004;265:462–477.
29 Manuel M, Georgala PA, Carr CB et al. Controlled overexpression of Pax6 in vivo negatively autoregulates the Pax6 locus, causing cell-autonomous defects of late cortical progenitor proliferation with little effect on cortical arealization. Development 2007;134: 545–555.
30 Beerens AMJ, Al Hadithy AFY,Rots MG et al. Protein transduction domains and their utility in gene therapy. Curr Gene Ther 2003;3:486–494.
31 Kristensen M, Birch D, Mørck Nielsen H. Applications and challenges for use of cell-penetrating peptides as delivery vectors for peptide and protein cargos. Int J Mol Sci 2016;17:185.
32 Freiermuth JL, Powell-Castilla IJ, Gallicano GI. Toward a CRISPR picture: Use of CRISPR/Cas9 to model diseases in human stem cells in vitro. J Cell Biochem 2018;119:62–68.


See www.StemCells.com for supporting information available online.

